Manifestation of Electrode Surface States in Molecular Conduction

Giorgos Fagas,*[1] *Rafael Gutierrez*,[2] *Klaus Richter*,[1] *Frank Grossmann*,[2] *Rüdiger Schmidt*[2]

[1] Institut für Theoretische Physik, Universität Regensburg, 93040 Regensburg, Germany
[2] Institut für Theoretische Physik, TU-Dresden, 01062 Dresden, Germany

Summary: We present a conduction mechanism across molecular junctions which derives from conductance resonances that are not associated with particular molecular orbitals. Instead, the resonances are induced by states localized at the surface of the electrodes. To this end, we studied the conductance of a C_{60} molecule bridging two carbon nanotubes. A simple tight-binding model is employed to investigate analytically the basic features of the effect.

Keywords: charge transport; fullerenes; Landauer theory; modeling; nanotechnology

Introduction: Molecules as Building Blocks for Electronic Circuits

Triggered by recent advances in chemical synthesis, scanning probe microscopy and break junction techniques, the seminal idea of using molecular-scale conductors as active components of electronic devices has received a new impulse.[1] Rectification, nanomechanical oscillators as well as negative differential resistance have already been demonstrated at the nanoscale.[2]

The understanding of the basic physical mechanisms that determine electron transport at the nanoscale is essential for achieving conductance control and, thus, for opening the possibility of device applications. Detailed studies at either the semiempirical or first-principles level have related the conduction mechanisms to the molecular electronic structure, the topology of the molecule/electrodes interface, charging effects, the band lineup and inelastic effects in long molecular wires.

Recently, we have studied molecular junctions which include mesoscopic electrodes such as carbon nanotubes (CNTs).[3-5] We have suggested a setup where a C_{60} molecule is contacted to two CNTs as an effective all-carbon molecular switch by molecular rotation.[4] An essential feature of such devices is the existence of localized electronic states at the electrode surface.[5]

 DOI: 10.1002/masy.200450810

Such states have important consequences in the electronic response of the junction and may in general be manifested in similar systems. An example includes localized states of anchor groups in a electrode/molecular wire/electrode bridge. Our approach is based on a combination of the Landauer theory of electronic transport with a tractable density-functional (DF) parametrized tight-binding Hamiltonian for calculating the electronic structure.

In the next section we present the theoretical method. Then the influence of surface states of the electrodes on the conductance of a CNT/C_{60}/CNT device is discussed. To reveal the effect, we compare with a simple tight-binding model followed by some concluding remarks.

Methodology: Landauer approach and Electronic Structure

We have recently developed an efficient method to calculate the conductance of two-terminal devices on the nanoscale.[5] The formulation is based on supplementing the Landauer picture of electronic transport with a density-functional parameterized tight-binding (DF-TB) approach to the electronic structure of the nanodevice. As shown in Figure 1, the device can be partitioned into three regions: two ideal (left and right) electrodes and a scattering region which includes the physical object of interest (e.g. molecule, cluster, nanowire) and, in most cases, some group of atoms belonging to the electrodes. The latter is particularly important when the electrodes' surface undergoes a structural relaxation which would introduce additional scattering. In this section the term 'molecule' is used to denote the scattering region.

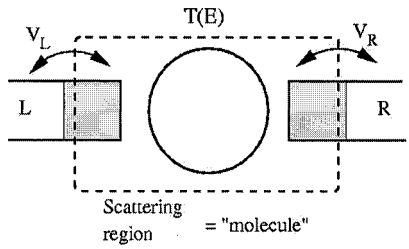

Figure 1. Schematic representation of a two-terminal device. The scattering region (enclosed in the dashed-line frame) with transmission probability *T(E)* is connected to semi-infinite left (L) and right (R) electrodes.

The Landauer approach[6] then reduces the calculation of the conductance *G* to the determination

of the transmission function *T(E)* within an elastic scattering problem of independent electrons with energy *E*. The relation in the linear regime at zero temperature is

$$G = \frac{e^2}{\pi\hbar} T(E_F) \tag{1}$$

where E_F is the equilibrium Fermi energy. Using Green functions techniques $T(E_F)$ is expressed as[7]

$$T(E_F) = Tr\left[G_M(E_F - i\eta)\Gamma_L(E_F)G_M(E_F + i\eta)\Gamma_R(E_F)\right] \tag{2}$$

In Equation 2, G_M is the Green function of the scattering region while $\Gamma_{L(R)}$ describe its effective coupling to the electrodes as described below.

From the Green function of the complete system it is possible to extract G_M using projector operator techniques.[8] The above mentioned partition of the setup leads to the following block representation of the full Hamiltonian matrix (in some suitable basis representation)

$$H = \begin{pmatrix} H_L & V_{L-M} & 0 \\ V_{L-M}^+ & H_M & V_{R-M} \\ 0 & V_{R-M}^+ & H_R \end{pmatrix} \tag{3}$$

The matrices $V_{L\text{-}M(R\text{-}M)}$ couple atoms belonging to the left (right) electrode to the molecule, and no direct coupling between the electrodes is assumed. Note that $H_{L(R)}$ are infinite dimensional submatrices. By projecting onto the molecular subspace via a projector P_M, it can be shown that G_M=P_M G P_M satisfies the M-dimensional matrix equation

$$(zS_M - H_M - \Sigma_L(z) - \Sigma_R(z))G_M(z) = 1; \qquad z = E + i\eta;\ \eta \to 0^+ \tag{4}$$

where S_M is the overlap matrix for the general case of a non-orthogonal basis set. The self-energies $\Sigma_{L(R)}$ include the coupling to the electrodes as well as information on their electronic structure. They are given by

$$\Sigma_{L(R)}(z) = (zS_{L(R)-M}^+ - V_{L(R)-M}^+)g_{L(R)}(z)(zS_{L(R)-M} - V_{L(R)-M}) \tag{5}$$

$S_{L(R)}$ are overlap matrices between orbitals centered on molecule and electrode atoms, and $g_{L(R)}$ (z) are electrode Green functions which are calculated using recursive techniques. Since the coupling matrices are in general short-range, they eliminate all contributions coming from atoms other than those nearest to the molecule. Hence, only surface Green functions are needed. Finally, the quantities $\Gamma_{L(R)}$ in Eq. 2 are given by i[$\Sigma_{L(R)}$(E+iη)-$\Sigma_{L(R)}$(E-iη)].

Then, the issue of characterizing the electronic structure of the molecule as well as that of the electrodes when treating real systems has to be considered. The DF-parameterized TB approach[9] relies on a representation of the single-particle electronic Kohn-Sham eigenstates ψ_i of the system within a non-orthogonal basis set $\varphi_\alpha(\mathbf{r}-\mathbf{R}_\alpha)$ taken as a valence basis localized at the ionic positions $\mathbf{R}_\alpha$, namely

$$\psi_i(\mathbf{r}) = \sum_\alpha c_\alpha^i \varphi_\alpha(\mathbf{r} - \mathbf{R}_\alpha) \tag{6}$$

With this *Ansatz* the Kohn-Sham equations for ψ_i are transformed into a set of algebraic equations

$$\sum_\beta (H_{\alpha\beta}^{\mathrm{TB}} - S_{\alpha\beta}E_i)c_\beta^i = 0 \tag{7}$$

In this expression the many-body Hamiltonian has been additionally approximated by a two-center (tight-binding) Hamiltonian H^{TB}, and $S_{\alpha\beta}$ is the corresponding overlap matrix. Note that the formal structure of Eq. 7 is that of the Hückel Hamiltonian. In contrast to the latter, however, all necessary matrix elements are calculated numerically using the φ_α-basis, which allows us to avoid the introduction of any empirical parameters. [9]

Results: electrode surface states and molecular conduction

In this section we demonstrate an unconventional way of metallization of a molecular bridge via intrinsic electrode surface states, which manifests itself as conductance resonances within the molecular HOMO-LUMO gap. As an example we utilize the molecular junction shown in Figure 2. We consider a C_{60} molecule between two semi-infinite *capped* metallic (5,5) CNTs. The diameters of the CNTs and the fullerene are comparable (~ 0.7 nm). The center of the fullerene is placed at the mid-point between the two pentagons at the cap-edges.

Because the molecular junction under discussion is a non-periodic system, we simulate it as a supercell with open boundary conditions. In addition to the caps, the CNT part consists of eight unit cells. The CNT back-bonds were saturated with hydrogens in order to avoid nonphysical charge transfer towards the nanotube caps. The scattering region includes the C_{60} molecule, the caps and the nearest-lying nanotube unit cells. A minimal basis set consisting of the 2s2p valence orbitals of carbon and the 1s orbital of hydrogen was used in the calculations. Due to the proximity of both subsystems (the cap-molecule separation is about 0.2 nm) the C_{60} cage is

expected to be slightly distorted. To take into account these modifications, we perform a structural optimization prior to each conductance calculation. Hereby we keep fixed all other unit cells that do not belong to the scattering region to simulate the bulk of the electrodes. It turns out that C_{60} adopts an ellipsoidal shape with its longer axis perpendicular to the transport direction.

A very important point is the determination of the equilibrium Fermi energy E_F of the whole system. As a first approximation, we have used the HOMO level obtained by diagonalizing the Hamiltonian matrix of the supercell after structural optimization of the molecular junction. With increasing supercell size, this level converges to the equilibrium Fermi level. We have tested that, with the cell size used in these calculations, the error in the Fermi energy lies within the precision of the DFTB method.

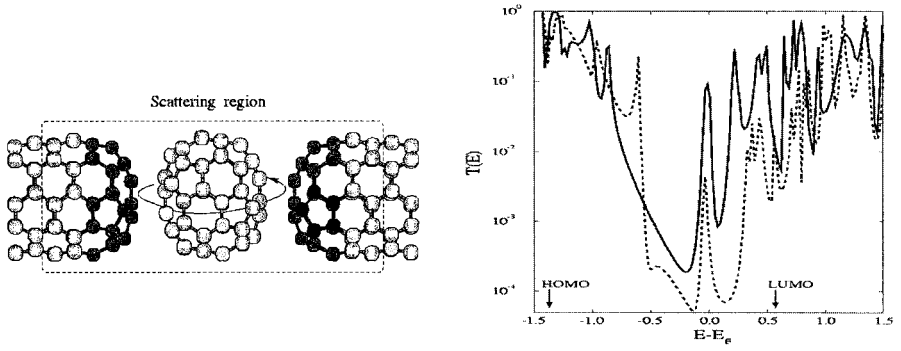

Figure 2: Geometric configuration of an all-carbon molecular junction (left). A C_{60} molecule bridges two (5,5) CNTs. Transmission spectra for two different molecular orientations (right). The HOMO and LUMO levels of the isolated C_{60} are indicated by arrows. Note the resonance at the Fermi energy.

Three features of this molecular junction should be highlighted:

(i) It is an all-carbon device, which means that large charge-transfer effects at equilibrium between the electrodes and the molecule can be ruled out. This is also supported by a Mulliken population analysis showing a very small charge accumulation on the molecule.

(ii) The lateral dimensions of the electrodes are of the same order as of the molecule. Thus, modifications of the interfacial atomic structure (produced, e.g., by some extrinsic mechanism like rotation or compression of the molecule) should strongly

influence the electronic conductance.[3-5]

(iii) The presence of topological defects (pentagons) on the electrode contact surfaces (caps) induces localized states around the equilibrium Fermi energy.[11] It is just this aspect that is related to the unconventional metallization of the molecule.

A typical transmission spectrum for two different orientations of C_{60} is shown in Figure 2 (lower panel). The rather strong variation of the peak intensities around the HOMO-LUMO gap is a direct consequence of point (ii) above and is thus related to modifications of the molecule/electrode interfacial coupling upon rotation.

Metallization by the electrode surface states is manifested by the conductance resonance near the Fermi energy. Its position and width remain nearly unaffected by molecular rotations, although its height strongly fluctuates. Since charge transfer is excluded, this resonance cannot be associated with a molecular orbital. Therefore, it is attributed to the states localized at the tips (caps) of the CNTs; see point (iii) above.

The basic features of the conductance around the Fermi energy described above can be nicely illustrated by considering a simple model Hamiltonian, schematically depicted in Figure 3. It consists of a dimer with hopping matrix element Γ coupled to two semi-infinite chains, which represent the electrodes. All atoms have a common onsite energy ε_0. A central feature of the model is the ability to trigger the presence of a localized state at the chain ends ('surface' state) which couples to the dimer and to the semi-infinite chains via parameters γ and $\gamma_{L(R)}$, respectively. The Hamiltonian reads

$$\begin{aligned} H &= H_{\mathrm{L}} + H_{\mathrm{R}} + H_{\mathrm{dimer}} + H_{\mathrm{surface}} \\ &= \varepsilon_0 \sum_{L,R} c_i^+ c_i + \beta \sum_{i=-\infty}^{0} (c_{i-1}^+ c_i + h.c.) + \beta \sum_{i=5}^{\infty} (c_{i-1}^+ c_i + h.c.) + \\ &\quad \varepsilon_0 \sum_{\mathrm{dimer}} c_i^+ c_i + \Gamma (c_2^+ c_3 + h.c.) + \gamma (c_1^+ c_2 + c_3^+ c_4 + h.c.) + \\ &\quad \varepsilon_0 \sum_{\mathrm{surface}} c_i^+ c_i + \gamma_L (c_0^+ c_1 + h.c.) + \gamma_R (c_4^+ c_5 + h.c.) \end{aligned} \tag{8}$$

where the subscripts 2,3 and 1,4 correspond to the dimer and the surface atoms, respectively.

For this model Eq. 2 simplifies to

$$T(\eta) = 4\kappa^2 \Delta_{\mathrm{L}}(\eta) \Delta_{\mathrm{R}}(\eta) |G_{14}(\eta)|^2 \tag{9}$$

where the Green function matrix element is given by

$$G_{14}(\eta) = \frac{\left(\lambda/\kappa\right)^2}{(2\kappa\eta - 1)(2\kappa\eta + 1)(2\cdot\eta - \Sigma_R(\eta))(-2\cdot\eta + \Sigma_L(\eta))} \qquad (10)$$

and

$$\Sigma_{L(R)}(\eta) = \Lambda_{L(R)}(\eta) - i\Delta_{L(R)}(\eta) = \mu_{L(R)}{}^2\left(\eta - i\sqrt{1-\eta^2}\right); \qquad |\eta| < 1 \qquad (11).$$

In deriving Eqs 9-11 we have introduced the following parametrization: $\beta/\Gamma=\kappa$, $\gamma/\Gamma=\lambda$, $\gamma_{L(R)}/\beta=\mu_{L(R)}$ and $\eta=-(E-\varepsilon_0)/2\beta$; the condition $|\eta|<1$ fixes the energy within the electrode band. Additionally, we have assumed that the coupling between the surface state and the dimer is weak ($\lambda<<1$), so that in the denominator of the G_{14}, all terms higher than first-order in λ have been neglected. This condition naturally arises if the molecular states are to be only slightly perturbed by the coupling to the electrodes. One clearly sees the pole structure of the Green function. Note that the dimer interacts only indirectly with the electrodes via the surface states and, hence, its HOMO ($\kappa\eta=-0.5$) and LUMO ($\kappa\eta=0.5$) are broadened by the electrodes only to (the neglected) second order in λ. To simulate a surface state, $\mu_{L(R)}$ should also be much smaller than unity.

To test our approximation, we compare in the left panel of Figure 3 the exact transmission function to that obtained from the above approximated expressions Eqs 9-11 in the limit of weak coupling. As can be seen, both curves are almost identical showing that Eq. 10 is a valuable approximation in this regime. Evidently, for $\mu_{L(R)}<<1$, the surface states correspond to the degenerate resonance at $\eta=0$ whose height is less than unity due to the asymmetric coupling to the electrodes. For weak coupling the latter is determined by $\lambda/\mu(=\mu_{L(R)})$.

By varying the surface state/molecule coupling, the width of the resonance is rather insensitive but the height is strongly modified in a similar fashion to our results on the CNT/C_{60}/CNT molecular junction. This is shown in the right panel of Figure 3. This follows from Eq. 10 which implies a λ–independent broadening and a height proportional to $(\lambda/\mu)^4$.

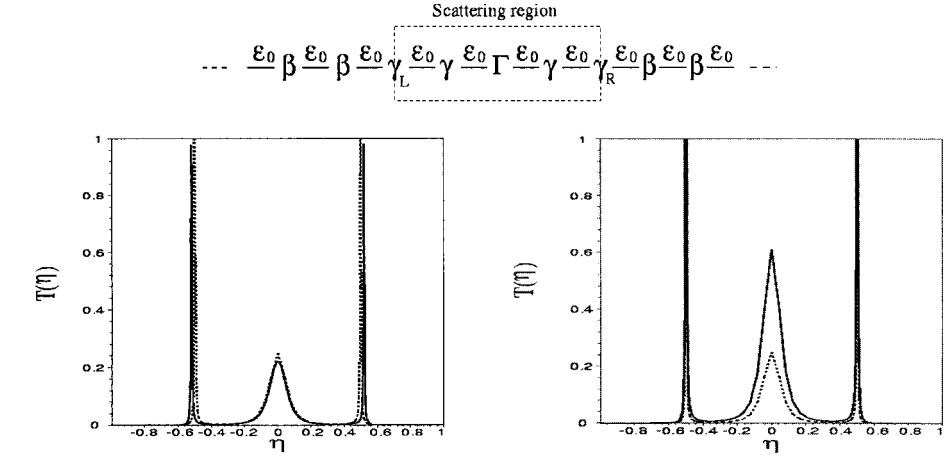

Figure 3.Upper panel: tight-binding model used to illustrate the conductance resonance induced by electrode surface states as found in the carbon-based molecular junction of Fig. 2. Lower panel: typical transmission function in the weak coupling regime as defined in the text. The resonance at zero arises from the electrodes. Left figure shows the comparison between the exact result and the weak coupling formula, Eqs 9-11. Here, κ=1, $\mu_{L(R)}$=0.4 and λ =0.2. Right figure illustrates the evolution of the resonance with respect to the coupling between the dimer and the electrode (λ equals 0.2 and 0.275 for the dashed and solid curve, respectively).

Concluding Remarks

By employing a novel molecular device, we pointed out the manifestation of surface resonant states of the electrodes in the conductance of molecular junctions. This presents an alternative way to metallization of a molecule and contrasts to the adopted view that electron transport across molecular junctions is simply dominated by hybridization of the molecular orbitals. The resulting conductance profile is generic to the appearance of surface resonant states within the HOMO-LUMO gap with characteristic additional resonances in this spectral window. To illustrate the effect, we analyzed a simple tight-binding model which reproduces all basic features. Moreover, in many setups anchor groups are used to bind the molecular bridge to the electrodes. These may also possess localized states with similar properties as the ones discussed in this paper. As pointed out,[12] sulfur atoms in thiol end groups offer such an example.

Acknowledgments

We would like to thank the organizers of the 2002 Prague Meeting on Macromolecules 'Electrical and Related Properties of Polymers and Other Organic Solids' for giving us the opportunity to present this work. Rafael Gutierrez acknowledges support by the Deutsche Forschungsgemeinschaft through the Forschergruppe 'Nanostrukturierte Funktionselemente in makroskopischen Systemen'. Giorgos Fagas is grateful to the Alexander von Humboldt Stiftung.

[1] A. Aviram and M. Ratner, *Chem. Phys. Lett.* **1974**, *29*, 277
[2] A. Aviram, M. Ratner, and V. Mujica (Eds), *Molecular Electronics II*, *Ann. N.Y. Acad. Sci.* **2002**, *960*; C. Joachim, J. K. Gimzewski, and A. Aviram, *Nature (London)* **2000**, *408*, 541
[3] G. Fagas, G. Cuniberti, and K. Richter, *Phys. Rev. B* **2001**, *63*, 045216; G. Cuniberti, G. Fagas, and K. Richter, *Chem. Phys.* **2002**, *281*, 465
[4] R. Gutierrez, G. Fagas, G. Cuniberti, F. Grossmann, R. Schmidt, and K. Richter, *Phys. Rev. B* **2002**, *65*, 113410
[5] R. Gutierrez, G. Fagas, K. Richter, F. Grossmann, and R. Schmidt, to be published in *Europhys. Lett.*
[6] R. Gutierrez, F. Grossmann, O. Knospe, and R. Schmidt, *Phys. Rev. A* **2001**, *64*, 0132
[7] S. Datta, *Electronic transport in mesoscopic systems*, Cambridge University Press, **1995**
[8] Y. Meir and N. S. Wingreen, *Phys. Rev. Lett.* **1992**, *68*, 2512
[9] P. O. Löwdin, *J. Chem. Phys.* **1951**, *19*, 1396
[10] O. Knospe, R. Schmidt, and G. Seifert, *Advances in Classical Trajectory Methods* **1999**, *4*, 153; Th. Frauenheim, G. Seifert, M. Elstner, Z. Hajnal, G. Jungnickel, D. Porezag, S. Suhai, R. Scholz, *Phys. Status Solidi (b)* **2000**, *217*, 41
[11] R. Tamura and M. Tsukada, *Phys. Rev. B* **1995**, *52*, 6015; D. L. Carroll *et al*, *Phys. Rev. Lett.* **1997**, *78*, 281
[12] J.K. Tomfohr and O. F. Sankey, *Phys. Rev. B* **2002**, *65*, 245105